Emergence of state at Fermi level due to the formation of In-Sn heterodimers on Si(100)-2 × 1

P. Sobotík,* M. Setvín, P. Zimmermann, P. Kocán, and I. Ošt'ádal
Charles University in Prague, Faculty of Mathematics and Physics, Department of Plasma and Surface Science, V Holešovičkách 2, 180 00 Praha 8, Czech Republic

P. Mutombo, M. Ondráček, and P. Jelínek
Institute of Physics, Academy of Sciences of the Czech Republic, Cukrovarnická 10, 162 00 Praha 6, Czech Republic
(Received 20 May 2013; revised manuscript received 20 August 2013; published 7 November 2013)

Structure and electronic properties of one-dimensional bimetallic In-Sn chains formed by codeposition on a Si(100)-2×1 surface are studied experimentally by means of scanning tunneling microscopy (STM) and scanning tunneling spectroscopy and theoretically using density-functional theory. The codeposition of In with a small amount of Sn allows separation of various In-Sn structures and their identification in empty-state STM images. A 16 × 2 supercell is employed to model an indium atomic chain in which one or two Sn atoms are embedded. This atomic model is used to identify unambiguously various In-Sn structures observed experimentally. At low Sn:In ratio the codeposition results in strongly preferential formation of isolated heterogeneous In-Sn dimers. The In-Sn dimer induces tilting of the neighboring homogeneous In-In dimer accompanied with a charge transfer. Consequently a localized state at Fermi level appears. These results contribute to a discussion on possible transport of electric charge along one-dimensional atomic chains of metals.

DOI: 10.1103/PhysRevB.88.205406 PACS number(s): 73.21.−b, 81.07.−b

I. INTRODUCTION

Nowadays surface characterization tools like scanning tunneling microscopy (STM) and atomic force microscopy (AFM) allow probing nanostructures locally, with atomic resolution. Thus it is possible to see an influence of a single atom on the structure properties and to study how the exchange of a particular atom by another type of atom influences local properties of the structure. Thus, an impact of single atom doping on local electronic properties of nanostructures[1] can be studied. Here we explore an influence of Sn atoms on electronic properties of one-dimensional (1D) semiconducting chains formed from In atoms on a Si(100)-2×1 surface using a combination of scanning tunneling microscopy and scanning tunneling spectroscopy measurements (STM/STS) and density-functional theory (DFT) calculations. We address structural and electronic features which have not been yet sufficiently studied.

The technologically important surface Si(100)-2×1 attracts attention as a natural template for self-assembled growth of truly one-dimensional structures, dimer chains of group-III and -IV metals which grow perpendicularly to silicon dimer rows.[2–5] A chain growth scenario has been already explained by a surface polymerization reaction.[6] It has been shown that these chains are not metallic; their electronic structure exhibits a surface-state band gap.[7–10] It has been suggested[7] that chains of heterogeneous In-Sn dimers might exhibit metallic conductivity. Stability of such chains was tested and reported in Refs. 11–13. In Ref. 11 the authors studied In-Sn (≈1:1) chains by STM and *ab initio* calculations and stated that codeposition of In and Sn results in formation of alternating In-In Sn-Sn homodimers in a chain. This conclusion was based on total-energy calculations of 2 × 2 structures (single dimers only). However, in their most recent paper[13] the authors reinterpreted STM observations and finally concluded that bright dots observed in filled-state STM images can be also explained by an antisymmetric configuration In-Sn Sn-In of two heterogeneous dimers and that a charge transfer between the two dimers results in a nonmetallic chain (as predicted by the theory of 1D systems[14]). However, electronic properties of particular dimers or dimer sequences observed in the bimetallic In-Sn chains have not been characterized either by atomically resolved scanning tunneling spectroscopy (STS) or theoretically by local density of states (LDOS) calculations. Moreover, a reliable interpretation of STM imaging of heterogeneous chains has not been reported yet. Recently, a theoretical study of mixed dimers and trimers composed of another combination of group-III and -IV metals—Al and Pb—was reported,[15] and metallic character of the dimers was predicted.

In our paper, we give a detailed atomically resolved interpretation of various structures observed in STM images of In-Sn bimetallic chains. A low In:Sn ratio results in localized In-Sn structures separated by chain segments composed of homogeneous In-In dimers. This allows us to resolve them using STM imaging and STS measurements. Large model structures of chains (up to 16 × 2) are used for DFT calculations of structure and density of states (LDOS) and for interpretation of experimental STM and STS data. Strong preference of forming isolated heterogeneous In-Sn dimers was observed at the low ratio Sn:In codeposition. The In-Sn dimer is stabilized by a charge transfer to the neighboring tilted In homogeneous dimer. Consequently a localized state at Fermi level arises. We demonstrate an existence of partially filled electronic states within such a semiconducting atomic chain and a chance to create a sequence of such states.

II. EXPERIMENTAL

STM measurements were performed at room temperature (RT) in a noncommercial ultra-high-vacuum STM system. The pressure in the system did not exceed 1×10^{-8} Pa during experiments. Si(100) substrates (Sb doped, *n*-type, resistivity $\leqslant 0.014\ \Omega$ cm) were used. To obtain the (2 × 1) reconstructed

 ©2013 American Physical Society

surface, the sample was several times flashed by dc current for ≈20 s to 1200 °C. In and Sn were deposited from tungsten wire evaporators, and evaporation rate was controlled by a quartz-crystal thickness monitor. The sample was resistively heated during the deposition by passing dc current, and the sample temperature was determined from calibrated heating power. STM tips were prepared by electrochemical etching from a polycrystalline tungsten wire and treated *in situ* on a Pt single crystal to ensure a metallic character of the tip and reproducible STS results. The dI/dV curves were measured using a lock-in technique (≈10 s per spectrum), and the presented data were averaged over several equivalent spectra normalized by I/V. Noise near the Fermi level was suppressed by a procedure from Ref. 16. A precise position of the STS measurement was marked in the corresponding STM image. To improve a dynamic range during the spectra measurement, we use a technique of a continuously varying tip-sample separation[17] $s = s_0 + a\,|V_s|$, where V_s is sample bias varying during the measurement and $a = 0.1 \div 0.2$ nm/V. A thermal drift was electronically compensated in all three axes.

To assure credibility of measured characteristics, we alternated the measurement on metal chains and on the clean silicon surface.

III. THEORETICAL METHODS

The theoretical results presented in the paper are based on DFT calculations within the local-density approximation (LDA)[18] using the FIREBALL code,[19,20] a molecular-dynamics DFT code based on local-atomic-orbital basis formalism. To simulate the Si(100) surface, we used a slab of eight layers passivated by hydrogen atoms at the bottom. Both hydrogen and the last Si layers were kept fixed during the structural relaxation until the Hellman-Feynman forces were smaller then 0.05 eV/Å and the difference in total energy dropped below 10^{-4} eV. To determine the most stable configuration among various structures of In-Sn heterodimers, 4×2 and 4×4 supercells were employed. Two (in a 4×2 unit cell) and four (in a 4×4 unit cell) heterodimers were used to model different configurations. A 16×2 supercell was employed to simulate an eight-dimers-long atomic chain. Sixteen k points were used for the integration in the Brillouin zone. We have used a well-tested basis set[21] containing s, p, and d orbitals for Si, In, and Sn atoms and s orbitals for H atoms. The following cutoff radii were employed: Si-Rc(Si,s) = 4.8 a.u., Rc(Si,p) = 5.4 a.u., Rc(Si,d) = 5.2 a.u.; H-Rc(H,s) = 3.8 a.u.; In-Rc(In,s) = 5.2 a.u., Rc(In,p) = 6.0 a.u, Rc(In,d) = 5.8 a.u.; Sn-Rc(Sn,s) = 5.2 a.u., Rc(Sn,p) = 5.7 a.u., Rc(Sn,d) = 5.6 a.u. Simulations of STM images were based on the Keldysh Green's-function formalism.[22] Calculations of the tunneling current were performed using a tungsten tip, made up of five atoms forming a pyramid connected to a (001) oriented tungsten slab. The electronic structure of the tip and tip-substrate hopping interactions were calculated within the FIREBALL formalism.[23,24] All calculations were done for a constant-height mode with an initial tip-sample separation of 5 Å to avoid any strong tip-sample interaction. In order to calculate tunnel spectra, we employed a so-called flat tip: a W tip with (artificially imposed) constant density of states. Its use is necessary to minimize the influence of the real density of states of the W cluster used as a tip. Alternatively, we used also a W tip with a Si atom at the apex. In this case we simulate a possible tip contamination by a Si atom. All calculations of I-V curves were done by placing a tip 5 Å above an atom. To characterize a dimer, the calculated currents over both dimer atoms were averaged. The dI/dV curves were then normalized by I/V.

IV. RESULTS AND DISCUSSION

Morphology of bimetallic In-Sn chains grown at a coverage of approximately 0.1 ML (1 ML = 6.87×10^{14} atoms/cm^2) at RT and 200 °C is shown in Fig. 1. The defects most frequently presented on the Si(100)-2×1 surface are also visible—missing dimers and C-type defects. They limit chain length, but their presence at given concentration is not important for our study. No significant segregation of the two components (i.e., growth of separated In and Sn chains) is observed. At RT, single isolated chains are formed. At 200 °C, a tendency to create clusters of chains is evident. The same tendency toward the two-dimensional clustering has been observed in the case of monometallic In chains. In filled-state images typical bright dots (see Ref. 11) within chains are clearly visible. Above 250 °C, In reacts with Si atoms and forms "magic" In-Si islands.[25] Our goal was to prepare relaxed structures and reduce the role of kinetics as much as possible. Therefore we have focused on a deposition temperature of 200 °C and a deposition rate of 0.005 ML/s.

In order to show different STM imaging of homogeneous In and Sn dimers, the In-Sn chains were prepared by separate deposition of Sn followed by In (see Fig. 2). No incorporation of In atoms into Sn chains was detected; only attachment of In at the chain ends was observed. In empty-state images, Sn

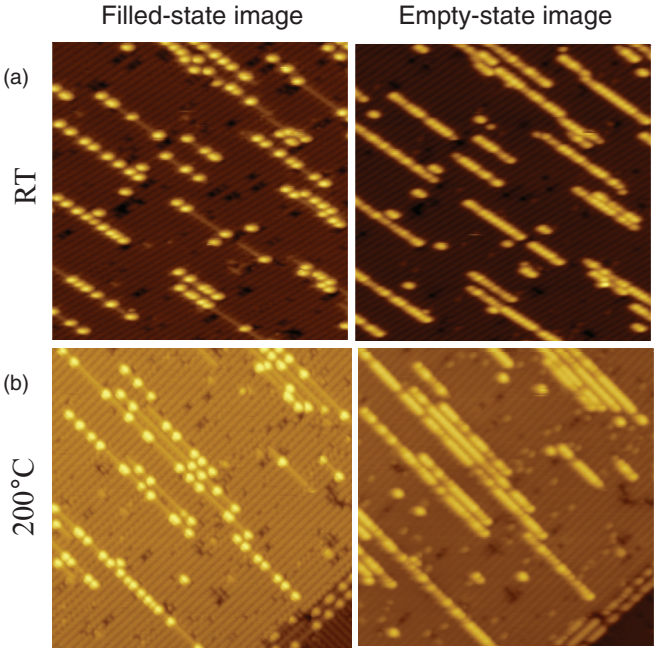

FIG. 1. (Color online) In-Sn chains prepared by codeposition at RT (a) and at 200 °C (b). Sn:In ratio, 1:3 (a) and 1:4 (b); area, 25 × 25 nm; tunneling conditions, $V_S = \pm 2$ V, $I_T = 300$ pA.

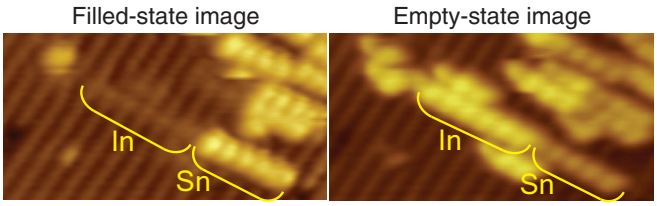

FIG. 2. (Color online) Subsequent deposition of Sn and In. Sn chains were prepared first by deposition at 200 °C. Then STM imaging started and In was deposited at RT during scanning. Area size, 5 × 10 nm; tunneling conditions, $V_S = \pm 2$ V, $I_T = 300$ pA.

chain segments appear slightly darker, but the contrast between the In and Sn parts is not so pronounced. In filled-state images, Sn parts of chains appear very bright in comparison to the In parts. Thus, In parts of chains can be identified easily in filled-state images, and consequently any bright dot in an In part of the chain reflects the presence of one or more Sn atoms (see Fig. 1). However, a precise composition of the observed objects cannot be determined from STM imaging only.

A. Classification of various In-Sn structures

We suppose that three types of metal dimers are basic building blocks of the studied dimer chains: homogeneous metal dimers composed of atoms of the same type—In-In or Sn-Sn—and heterogeneous In-Sn dimers with two possible orientations.

STM filled-state images of the chains with a relatively low amount of Sn (with a Sn:In ratio from 1:5 to 1:10) grown at temperatures $\leqslant$200 °C show the bright dots well separated between relatively long segments of indium chains [see Figs. 3(a) and 3(c)]. Such structures are suitable for interpretation of the observed bright dot objects because we can easily assign a particular bright dot to the corresponding structure observed in the empty-state image.

Figure 3 shows details of chains with a low Sn:In ratio (1:7). We can see that each bright dot object observed in filled-state images corresponds to a particular number of darker dimers visible in empty-state STM images [Fig. 3(e)]. Monometallic Sn or In chains appear uniform in empty and filled states. Since Sn chains appear relatively darker in empty states, we can assume that the darker dimers contain Sn atoms. According to the number of darker dimers related to a particular bright dot and also according to their height profiles shown in Figs. 4 and 5 we sort the observed objects to one-dimer (D_1 and D_2), two-dimer (TD), and three-dimer (THD) structures. We did not observe any single bright dot corresponding to a four-dimer structure or larger. Relative abundances of the observed structures within In chains are D_1, 48%; D_2, 3%; TD, 43%; and THD, 6% (cumulative chain length was about 1500 dimers, and chain ends were excluded).

In what follows, we will focus mainly on one- and two-dimer structures to identify In-Sn heterogeneous dimers.

B. Total-energy calculations of expected model structures

It has been already shown[13] that in the case of chains containing the same amounts of Sn and In a formation of heterodimers with antisymmetric In-Sn Sn-In ordering is

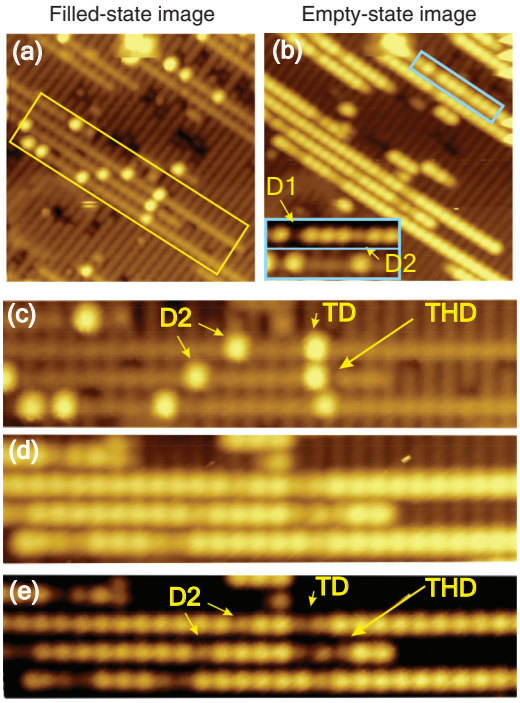

FIG. 3. (Color online) Details of single dimers and bright dots in In-Sn chains, with the initial part of the surface imaged in filled (a) and empty (b) states, size 15 × 15 nm^2. An area surrounded by the yellow rectangle in panel (a) is shown below as a filled-state image (c), an empty-state image (d), and a contrast-enhanced empty-state image (e). One-(D_1,D_2), two-(TD), and three-dimer (THD) structures are marked by arrows. Insertion in panel (b) shows empty- and filled-state images of the two different types of one-dimer structures in the chain segment marked by the rectangle. Sn:In ratio, 1:7; tunneling parameters, sample voltage ±2 V, tunneling current 50 pA.

strongly preferred (we adopt ordering notation introduced by Magaud *et al.* in Ref. 13, where also symmetric In-Sn In-Sn ordering was introduced). We obtained the same results for

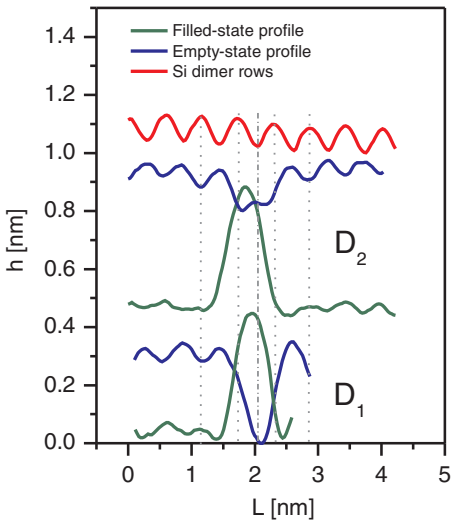

FIG. 4. (Color online) Profiles of various one-dimer structures, measured along In-Sn chains. A profile across Si dimer rows, parallel with chains, is shown for comparison. Tunneling conditions, $V_S = \pm 2$ V, $I_T = 50$ pA.

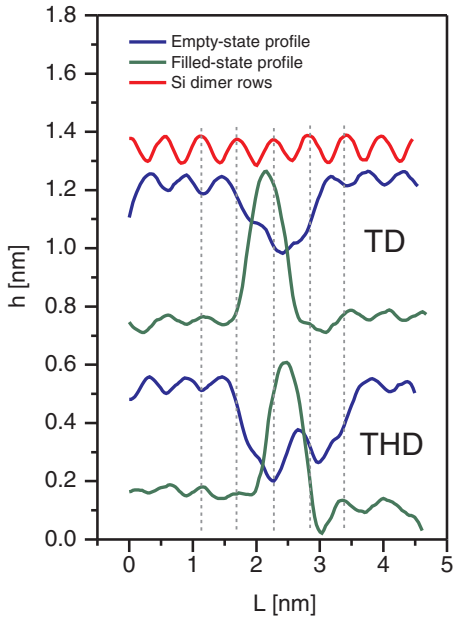

FIG. 5. (Color online) Profiles of two-dimer (TD) and three-dimer (THD) structures, taken along In-Sn chains. The profile taken across Si dimer rows (red) is shown for comparison. Dotted lines indicate positions of Si dimer rows. Tunneling conditions, $V_S = \pm 2$ V, $I_T = 50$ pA.

both 4 × 2 and 4 × 4 supercells (not shown here). However, to model single bright dots experimentally observed at a low Sn:In ratio we employed a 16 × 2 supercell representing an atomic chain eight dimers long. In order to evaluate the relative stability of expected one- and two-dimer structures embedded into In chains, we compared total energies calculated for these structures. Because such a direct comparison of total energies can be meaningfully made only if the numbers of In and Sn atoms are the same for all the different structures, pairs of 16 × 2 supercells were constructed in such a way that each pair contains 30 In and 2 Sn atoms. In the case of chains with two Sn atoms, the second chain in the pair was a monometallic In chain. In the case of a single Sn atom in a chain the pair consisted of two identical chains. The total energy of the whole system is simply taken to be the sum of the total energies calculated for both these 16 × 2 supercells. The results are shown in Table I. Having two Sn atoms in the two In chains, formation of two independent In-Sn heterodimers is preferred. The second most stable structure is an antisymmetric configuration of the two heterodimers. Also,

TABLE I. Total-energy calculations of various basic structures embedded in an indium chain. ΔE is related to the energy of a structure which consists of two 16 × 2 structures, one of which represents a monometallic In chain and one of which represents a Sn dimer in an indium chain [the structure in Fig. 6(a)].

2 × (16 × 2) configuration	ΔE (eV)
Single (Sn-Sn) dimer in In chain	0
Symmetric (In-Sn In-Sn) dimers in In chain	−0.09
Antisymmetric (In-Sn Sn-In) dimers in In chain	−0.31
Two independent (In-Sn) dimers in In chain	−0.38

a symmetric configuration of the heterogeneous dimers seems to be more stable than a Sn homogeneous dimer. The model structures are shown in Figs. 6 and 7 and will be discussed in the next sections. On the other hand, we should stress that also kinetics processes may strongly influence abundance of different In-Sn structures within nanowires.

C. One-dimer structures

Two different one-dimer structures were identified from STM images. They are marked as D_1 and D_2 in Fig. 3. The object D_1 appears relatively darker in empty-state images [Fig. 3(b), inset] compared to the D_2 object. Tunnel spectra measured above D_1 correspond well to those obtained on monometallic Sn chains [see Fig. 6(a)], so the D_1 object can be interpreted as a single Sn-Sn homodimer. Results of DFT calculations of the 16 × 2 model structure which consists of seven In dimers and one Sn homodimer confirm this assumption. The calculated relaxed structure containing the Sn homodimer is shown in the upper part of Fig. 6(a); the Sn-Sn dimer is tilted (the height difference of atoms in the dimer is $\Delta h = 0.85$ Å). The In-In dimer nearby the upper Sn atom is slightly tilted as well (the height difference of the two In atoms is $\Delta h = 0.13$ Å). The theoretical LDOS projected to adatoms, the calculated tunnel spectrum, and the STM image of the Sn dimer in an indium chain are shown in Fig. 6(a). The LDOS projected to individual Sn atoms in a dimer shows that the dimer buckling is accompanied by a charge transfer from the bottom Sn atom to the upper one.[13]

The second object D_2 is brighter than D_1 in empty-state images and appears slightly asymmetric [Fig. 3(b), inset]. The profile measured along the chain (see Fig. 4) shows that the bright dot in the filled-state image is not placed symmetrically between Si dimer rows. Considering an appearance of In-In and Sn-Sn homogeneous dimers, it is reasonable to interpret the object D_2 as an In-Sn heterodimer. Surprisingly, two different types of tunnel spectra were measured for the same imaged D_2 structures [Fig. 6(b)]. The *A*-type STS exhibits a surface-state band gap and significant increase just above the Fermi level. The *B*-type structure STS curve clearly exhibits nonzero value at the Fermi level and a minimum slightly above Fermi level, which indicates the presence of half-filled states at the Fermi level.

To shed light on this, the experimental data for the D_2 object were compared with DFT calculations performed for the model 16 × 2 structure containing a single In-Sn dimer and seven In-In dimers. The calculated relaxed structure shows tilting of the heterogeneous In-Sn dimer ($\Delta h = 0.85$ Å), with the upper Sn atom, and also significant tilting of the In dimer neighboring with the Sn atom of the mixed dimer ($\Delta h = 0.58$ Å). The In-In dimer on the opposite side of the mixed dimer is slightly tilted as well ($\Delta h = 0.04$ Å). The rest of the homogeneous In dimers in the structure are not tilted at all. The calculated LDOS [see Fig. 6(b)] exhibits states at the Fermi level. Magaud *et al.*[13] predicted the presence of a half-filled state at Fermi level localized at the heterogeneous dimer. However, our results show that the state appearing at the Fermi level is shifted to the neighboring homogeneous In dimer. Spatial distribution of this state is shown in Fig. 8(a). The main contribution to the state

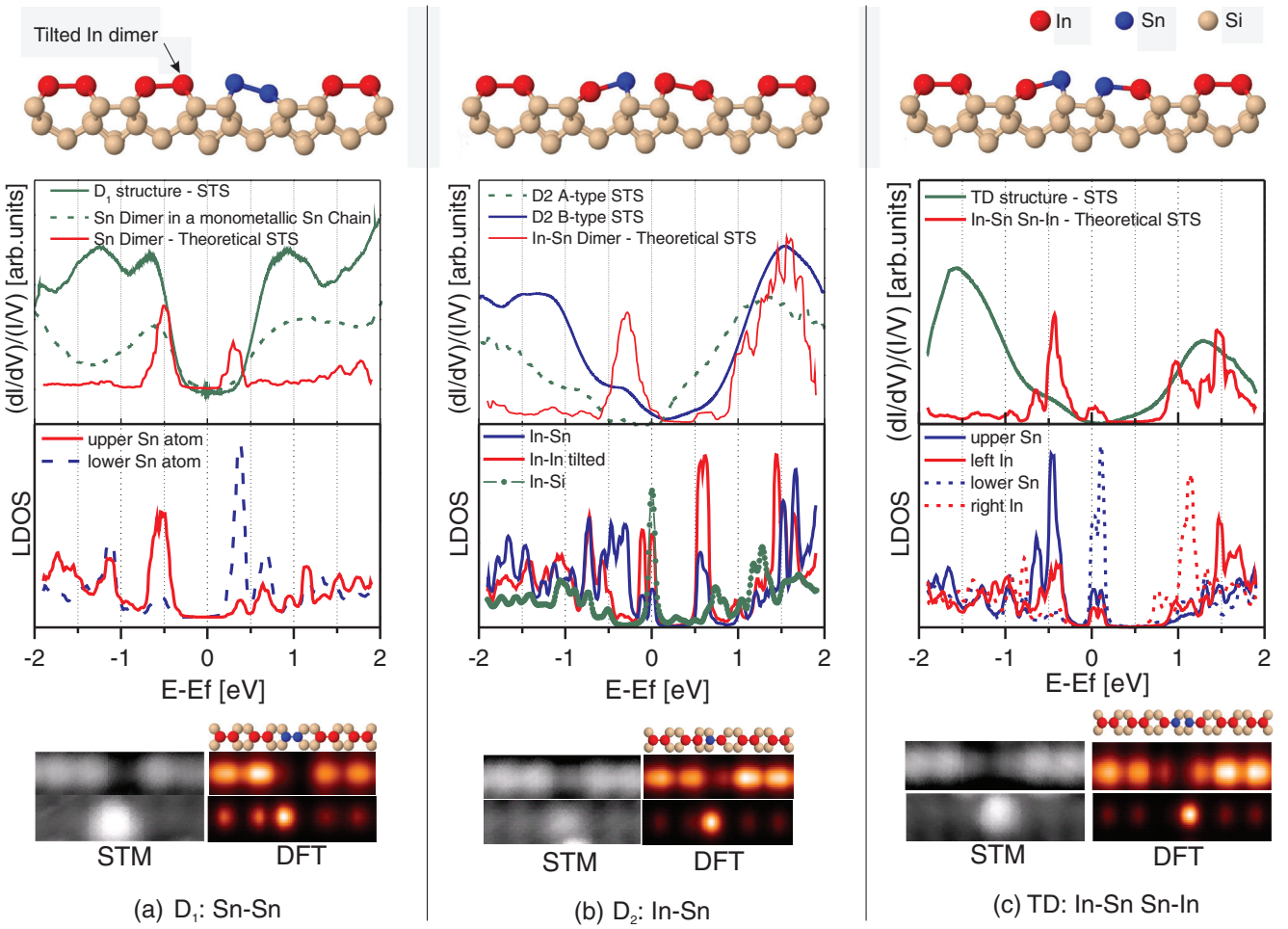

FIG. 6. (Color online) Model structures, calculated projected LDOS, theoretical STS curves, and STM images for Sn-Sn dimer (a), In-Sn dimer (b), and In-Sn Sn-In structure (c) in an indium chain, compared with STM images and tunnel spectra of D_1 (a), D_2 (b), and TD (c) structures.

comes from p_y orbitals forming a bond between In atoms. A comparison of the experimental STS curves measured above bright dots in filled-state images with the theoretical LDOS and calculated tunnel spectra shows that only the D_2 object characterized by the B-type STS curve is in agreement with the theoretical predictions for a single In-Sn heterodimer. The tunnel spectrum of the A-type structure exhibits a different feature—the small gap of 0.5 eV below the Fermi level. It has been shown recently[26] that there is a relatively large probability to find a Si atom instead of a Sn atom in chains deposited at 200 °C. Such an exchange may explain the different spectrum of the A-type structure, and the structure could be the In-Si heterogeneous dimer. It is also supported by theoretical LDOS for a In-Si dimer [shown in Fig. 6(b)] which clearly exhibits a small surface-state band gap of 0.5 eV below the Fermi level. However, the significant state visible in LDOS at Fermi level is

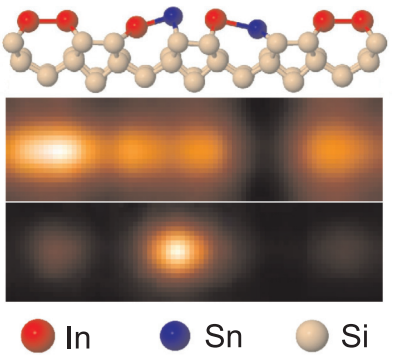

FIG. 7. (Color online) Theoretical structure and calculated STM image of In-Sn In-Sn dimers in an indium chain.

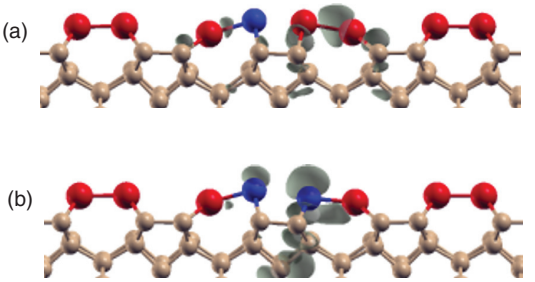

FIG. 8. (Color online) Spatial distribution of the state at Fermi level for a single In-Sn heterodimer (D_2) (a) and for the In-Sn Sn-In structure (TD) (b). Energy range, ±0.15 eV.

in the STS curve probably shifted slightly above Fermi level, where the sudden increase in STS is visible. The fact that agreement between presented STS data and theory is not perfect can be explained mainly by the unknown structure and composition of the real STM tip apex and the fact that STS measurements were performed at RT. Also, band bending and influence of the tip on the position of the probed atom[26] can cause a shift of the observed maxima.

D. Two-dimer structures

With respect to the interpretation of one-dimer structures (D_1 and D_2) and imaging of homogeneous indium and tin chains we can interpret the observed two-dimer structures either as an antisymmetric or symmetric configuration of two In-Sn heterodimers. The most stable and thus the most probable 2×4 structure is the antisymmetric In-Sn Sn-In structure. Also, the symmetry of the TD structure, well visible in line profiles in Fig. 5, corresponds to this structure. A comparison with the theoretical STM images of the two configurations confirms the expectation that the TD object represents the antisymmetric In-Sn Sn-In configuration of two heterogeneous dimers. Figure 6(c) shows the calculated relaxed structure of the In-Sn Sn-In dimers surrounded by six In dimers. The two heterodimers are tilted, both with Sn atoms up. The height difference in the left heterodimer with the higher Sn atom is $\Delta h = 0.79$ Å; the other one is less tilted with $\Delta h = 0.25$ Å. The In-In homogeneous dimers are untilted. According to the shown theoretical LDOS [Fig. 6(c)], the two neighboring heterogeneous In-Sn dimers exhibit different electronic properties compared to a single heterodimer. In agreement with Ref. 13 the In-Sn Sn-In structure is stabilized by a different tilting of the neighboring dimers accompanied with charge transfer from the lower to the upper Sn atom, resulting in semiconducting character of the structure. The contribution of particular Sn atoms to LDOS is shown in Fig. 6(c) too. While the peak at ≈ -0.5 eV in the filled states is related to the upper Sn atom, the empty-state peak ≈ 0.1 eV above Fermi level corresponds to the lower one. A gap of 0.6 eV appears. The states just above the Fermi level associated with the lower Sn atom are suppressed in experimental and partially in theoretical tunnel spectra. A contribution of the higher Sn atom to the tunnel signal dominates. A spatial distribution of the states close to the Fermi level is shown in Fig. 8(b). These states are strongly localized at Sn atoms, and thus an overlap with similar states in neighboring dimers is small. Consequently the chain composed of alternating In-Sn Sn-In structures probably will not be conducting, even if we somehow excite or inject electrons to the states just above Fermi level. The alternative symmetric configuration In-Sn In-Sn—shown in Fig. 7—was not recognized in our STM images.

E. Three-dimer structures

We also attempted to interpret the observed three-dimer (THD) structures. After comparison of the experimental and simulated STM images we concluded that the THD structure represents a configuration of two antisymmetric In-Sn and Sn-In heterodimers separated by the In-In dimer in the indium chain. Its model structure and comparison of theoretical and experimental STM images is shown in Fig. 9. An alternative symmetric In-Sn In-In In-Sn In-In structure will inevitably produce two bright dots in filled-state images, because the In-Sn heterodimer strongly influences only the neighboring dimer on its Sn side. The latter structure should thus appear as two clearly separated In-Sn dimers. We also tested other configurations, like In-Sn Sn-Sn Sn-In and In-Sn Sn-In In-Sn, but corresponding theoretical STM images did not fit to the experimental data. Although the THD structure consists of separated heterodimers, it does not exhibit states at the Fermi level as observed in the case of the single heterodimer In-Sn. The theoretical LDOS shows some states close to the Fermi level, which are again localized at the tilted In-In homodimer (not shown here). Thus, states at the Fermi level formerly localized at the tilted In-In homodimer in the case of a single heterodimer were shifted from the Fermi level due to the interaction with the second heterodimer.

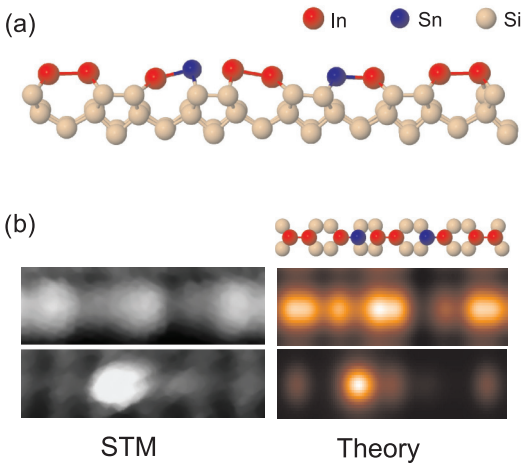

FIG. 9. (Color online) Structure of In-Sn In-In Sn-In dimers (a) and calculated and measured STM images (b).

F. Discussion

The presented low coverage low Sn:In ratio data suggest that codeposition of In and Sn atoms results in formation of In-Sn heterodimers. It has been directly observed in our STM experiment that the In-Sn heterodimers have a stabilizing effect and prevent a decay of In chains.[27] Homogeneous Sn-Sn dimers represent only 2% of the observed structures containing Sn atoms.

Incorporation of Si atoms has to be discussed as well. We have suggested already that the *A*-type D_2 structure is related to the presence of a single In-Si heterodimer. In Ref. 26 we showed from a noncontact AFM experiment that also two-dimer structures containing one Si atom instead of a Sn atom can be observed (In-Si Sn-In). Theoretical calculations gave practically the same LDOS for TD structures containing either Sn or Si atoms. Therefore it is difficult to resolve them from a STM/STS experiment, contrary to single In-Si and In-Sn heterodimers. We expect the same problem also for three-dimer structures.

We have shown that the presence of a single In-Sn dimer in an indium chain induces distortion—tilting of the In dimer

adjacent to the Sn atom. The distortion is accompanied by a charge transfer from the In homodimer to the In-Sn heterodimer and by filling of the dangling bond of the Sn atom. The missing charge causes emergence of a half-filled state localized at the bond between In atoms. Addition of another In-Sn dimer creates a more stable structure with the antisymmetric ordering of the adjacent heterogeneous dimers. In a similar way as in the previous case, tilting of the dimers is accompanied with a charge transfer from the one In-Sn dimer to the neighboring one. In this case one dangling bond is completely filled and the other one is empty, and the structure becomes semiconducting as predicted by Magaud *et al.*[13] Combination of two In-Sn heterodimers with a single In-In dimer in the three-dimer structure In-Sn In-In Sn-In results in tilting and charge transfer, where the second Sn-In dimer supplies an electron to fill the half-filled state at the tilted In-In dimer. The states at the Fermi level are shifted away, and the structure becomes semiconducting. In general, the isolated In-Sn In-In structure in an indium chain is metallic. From the fact that the next neighboring In dimer is not influenced significantly we estimate that single In-Sn dimers must be separated at least by two In homodimers to prevent an additional charge transfer. Otherwise, an interaction of formerly metallic In-Sn In-In structures, accompanied by dimer tilting and charge transfer to reduce the number of half-filled dangling bonds, will result in a metal-semiconductor transition analogous to the Peierls transition in a chain composed of single metal atoms with one electron per atom.[28]

V. CONCLUSIONS

We have studied formation of various bimetallic structures embedded into In chains on Si(100)-2×1 using STM/STS and DFT. The basic elementary structures, formed by codeposition at low Sn:In ratio, were distinguished and associated with the model structures. It has been shown that the bright dots in filled-state images, already reported in Refs. 11–13, are associated not only with one-dimer structures (which differ from homogeneous In-In dimers in an In chain) but also with structures composed of two or even three dimers. We have shown that formation of single heterodimers and double heterodimers with antisymmetric ordering is preferred. It has been demonstrated theoretically and experimentally that formation of the In-Sn heterogeneous dimer in an indium chain induces emergence of localized electronic states at, or slightly above, Fermi level.

ACKNOWLEDGMENTS

We wish to acknowledge the support of the Czech Science Foundation under Project No. P204/10/0952. P.M., P.J., and M.O. acknowledge the financial support of the Grant Agency of the Academy of Sciences of the Czech Republic under Project No. M100101207. M.O. acknowledges the support provided by the Czech Science Foundation under Project No. P204/11/P578. P.Z. acknowledges the financial support of the Grant Agency of Charles University under Projects No. 80010 and No. 122413.

*pavel.sobotik@mff.cuni.cz

[1] M. Fuechsle, J. A. Miwa, S. Mahapatr, O. W. H. Ryuand S. Lee, L. C. L. Hollenberg, G. Klimeck, and M. Y. Simmons, Nat. Nanotechnol. **7**, 242 (2012).
[2] A. A. Baski, J. Nogami, and C. F. Quate, J. Vac. Sci. Technol. A **8**, 245 (1990).
[3] J. Nogami, S. Park, and C. F. Quate, Appl. Phys. Lett. **53**, 2086 (1988).
[4] M. M. R. Evans and J. Nogami, Phys. Rev. B **59**, 7644 (1999).
[5] J. E. Northrup, M. C. Schabel, C. J. Karlsson, and R. I. G. Uhrberg, Phys. Rev. B **44**, 13799 (1991).
[6] G. Brocks, P. J. Kelly, and R. Car, Phys. Rev. Lett. **70**, 2786 (1993).
[7] Z.-C. Dong, T. Yakabe, D. Fujita, Q. D. Jiangand, and H. Nejo, Surf. Sci. **380**, 23 (1997).
[8] Z.-C. Dong, D. Fujita, and H. Nejoh, Phys. Rev. B **63**, 115402 (2001).
[9] K. Tono, H. W. Yeom, I. Matsuda, and T. Ohta, Phys. Rev. B **61**, 15866 (2000).
[10] H. W. Yeom, T. Abukawa, Y. Takakuwa, Y. Mori, T. Shimatani, A. Kakizaki, and S. Kono, Phys. Rev. B **53**, 1948 (1996).
[11] L. Juré, L. Magaud, P. Mallet, and J.-Y. Veuillen, Appl. Surf. Sci. **162-163**, 638 (2000).
[12] L. Magaud, A. Pasturel, L. Juré, P. Mallet, and J.-Y. Veuillen, Surf. Sci. **454–456**, 489 (2000).
[13] L. Magaud, A. Pasturel, and J.-Y. Veuillen, Phys. Rev. B **65**, 245306 (2002).
[14] *Density Waves in Solids*, Frontiers in Physics, edited by D. Pines (Addison-Wesley, Boston, 1994).
[15] A. Puchalska, A. Racis, L. Jurczyszyn, and M. W. Radny, Surf. Sci. **608**, 188 (2013).
[16] M. Prietsch, A. Samsavar, and R. Ludeke, Phys. Rev. B **43**, 11850 (1991).
[17] J. A. Stroscio and R. M. Feenstra, in *Scanning Tunneling Microscopy*, edited by J. A. Stroscio and W. J. Kaiser (Academic, San Diego, 1993).
[18] D. M. Ceperley and B. J. Alder, Phys. Rev. Lett. **45**, 566 (1980).
[19] P. Jelínek, H. Wang, J. P. Lewis, O. F. Sankey, and J. Ortega, Phys. Rev. B **71**, 235101 (2005).
[20] J. P. Lewis, P. Jelínek, J. Ortega, A. A. Demkov, D. G. Trabada, B. Haycock, H. Wang, G. Adams, J. K. Tomfohr, E. Abad, H. Wang, and D. A. Drabold, Phys. Status Solidi B **248**, 1989 (2011).
[21] M. Basanta, Y. Dappe, P. Jelínek, and J. Ortega, Comp. Mat. Sci. **39**, 759 (2007).
[22] J. M. Blanco, F. Flores, and R. Perez, Prog. Surf. Sci. **81**, 403 (2006).
[23] J. M. Blanco, C. Gonzalez, P. Jelínek, J. Ortega, F. Flores, and R. Perez, Phys. Rev. B **70**, 085405 (2004).
[24] J. M. Blanco, C. Gonzalez, P. Jelínek, J. Ortega, F. Flores, R. Perez, M. Rose, M. Salmeron, J. Mendez, J. Wintterlin, and G. Ertl, Phys. Rev. B **71**, 113402 (2005).
[25] V. G. Kotlyar, A. V. Zotov, A. A. Saranin, T. V. Kasyanova, M. A. Cherevik, O. V. Bekhtereva, M. Katayama, K. Oura, and V. G. Lifshits, J. Surf. Sci. Nanotechnol. **1**, 33 (2003).
[26] M. Setvín, P. Mutombo, M. Ondráček, Z. Majzik, M. Švec, V. Cháb, I. Ošt'ádal, P. Sobotík, and P. Jelínek, ACS Nano **6**, 6969 (2012).
[27] P. Kocan, L. Jurczyszyn, P. Sobotik, and I. Ostadal, Phys. Rev. B **77**, 113301 (2008).
[28] R. E. Peierls, *Quantum Theory of Solids*, 1st ed. (Oxford University Press, Oxford, 1955).